

# STUDIES OF ULTIMATE INTENSITY LIMITS FOR HIGH POWER PROTON LINACS

C. Plostinar, C. R. Prior, G. H. Rees, STFC/ASTeC/RAL, UK  
 S. L. Sheehy, JAI/University of Oxford and STFC/ASTeC/RAL, UK  
 I. V. Konoplev, A. Seryi, JAI/University of Oxford, UK  
 M-O. Boenig, A. Geisler, O. Heid, Siemens AG, DE

## Abstract

Although modern high power proton machines can now routinely deliver MW level operating powers, the next generation accelerators will be required to reach powers orders of magnitude higher [1,2]. Significant developments will be needed both in technology and in understanding the limits of high intensity operation. The present study investigates the beam dynamics in three experimental linac designs when the beam intensity is increased above current levels such that for CW regimes, beam powers of up to 400 MW can be attained. In the first, a 1 A proton beam is accelerated to 400 MeV using normal conducting structures. In the second, a comparison is made when two front ends accelerate 0.5 A beams to ~20 MeV where they are funnelled to 1 A and accelerated to 400 MeV. Similarly, in the third, two 0.25 A beams are funnelled to 0.5 A and then accelerated in superconducting structures to 800 MeV. In addition, alternative unconventional methods of generating high current beams are also discussed. The further studies that are needed to be undertaken in the future are outlined, but it is considered that the three linac configurations found are sufficiently promising for detailed technical designs to follow.

## INTRODUCTION

Achieving higher average proton beam powers at energies up to GeV level will require designing machines at much higher duty cycles as well as a significant increase in the beam current from the typical 0.1 A or less available today. This approach was first proposed for the APT project at LANL where a 1.7 GeV CW, 0.1 A linac was designed, aimed at delivering beam powers of up to 170 MW [3]. While increasing the beam intensity poses significant challenges both conceptual and technological, it can have the advantage of leading to shorter, more economical and much more efficient machines in terms of transferring grid power to beam power. The beam dynamics involved at the upper limits of intensity operation will be further examined.

## OPTION 1

The first linac option developed is a 400 MeV, 1 A normal conducting machine. Assuming CW operation this is equivalent to an output beam power of 400 MW. The design intensity is particularly challenging, as it is up to two orders of magnitude higher than most proton linacs in use today. For the purpose of this study, to investigate the beam dynamics of such a machine, potential limiting factors (ion

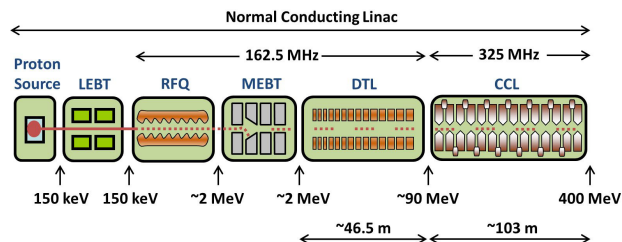


Figure 1: General layout of the 400 MeV, 1 A, normal conducting linac (Option 1).

source capabilities, cooling challenges, RF sources, beam loading, etc.) were overlooked, under the assumption that future technological progress can overcome most of these issues.

A schematic linac layout can be seen in Figure 1. It consists of a 2 MeV front end followed by a Drift Tube Linac (DTL) up to 90 MeV and a Coupled Cavity Linac (CCL) up to the final energy. The front end has a standard configuration with a proton source, Low Energy Beam Transport Line (LEBT), a Radiofrequency Quadrupole (RFQ) and a matching section to the DTL (MEBT). Previous work [4] on high intensity proton injectors indicated that for high beam currents a significant increase in the transverse beam size is expected and therefore larger aperture accelerating structures are essential. Consequently, the RFQ operating frequency is reduced to 162.5 MHz and is maintained up to the end of the DTL where it is doubled to 325 MHz. This allows an aperture radius of 30 mm in the DTL and CCL.

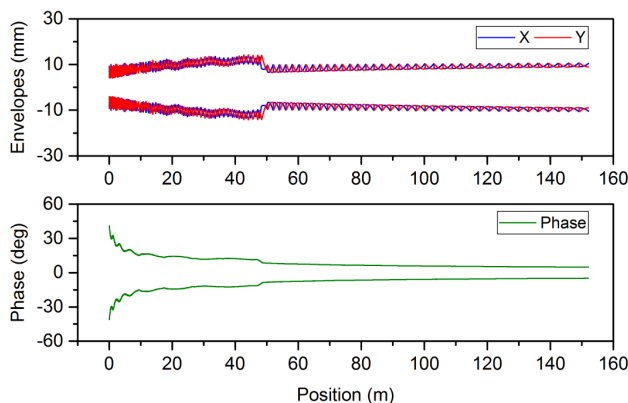


Figure 2: Beam envelopes in the Option 1 linac (2-400 MeV): horizontal (X), vertical (Y) and longitudinal (Phase).

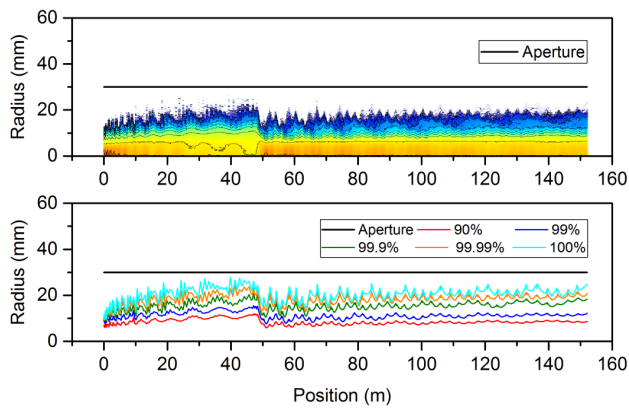


Figure 3: Radial beam density (top), and beam cross-section (bottom) evolution in the Option 1 linac (2-400 MeV).

The design of the accelerating structure presents several challenges. The choice of low frequency and larger apertures decreases the average shunt impedance to  $\sim 26$  MOhm/m. The total dissipated power for the five DTL tanks is  $\sim 9.6$  MW. The CCL consists of 39 cavities in an eight cell per cavity configuration and a total dissipated power of  $\sim 52$  MW. A particular difficulty at low energies is to capture the RFQ beam efficiently under heavy space charge conditions. Longitudinally this is done by adiabatically ramping the synchronous phase in the first DTL tank from  $-50$  to  $-30$  degrees. The accelerating gradient is also ramped from 3 to 4 MV/m. In the CCL, the synchronous phase is kept constant at  $-25$  degrees as well as the accelerating gradient at 4.5 MV/m.

For the beam dynamics, a FODO focusing lattice was adopted. A full parameter scan was further carried out to allow the optimal choice of tunes such that instabilities and resonant conditions are avoided. Meticulous initial matching is performed as well as at transitions, while ensuring a smooth evolution of phase advance throughout the entire linac. The result can be seen in Figure 2 where the full transverse and longitudinal envelopes are presented.

The design is also analysed by means of multi-particle simulations with 3D space charge using TraceWin [5] and Parmila [6]. The assumed starting conditions use high intensity tracking results in RFQs from existing studies [4]. For a 1 A beam, a DTL input RMS emittance of  $1.1 \pi$ .mm.mrad transversely and  $2.8 \pi$ .mm.mrad longitudinally is presumed. Figure 3 shows the resulting radial beam density, as well as the density level through the linac when tracking a uniform distribution with  $10^5$  macroparticles. It is immediately clear that the solution adopted leads to a well-contained beam, which remains within the 30 mm aperture radius for the entire acceleration. Although the beam halo occupies a large proportion of the beam pipe, no losses are observed. The initial particle charge density is more or less conserved and the tune depression kept constant at  $\sim 0.4$ . The total emittance growth is  $\sim 30\%$  transversely and  $\sim 10\%$  longitudinally. While this is encouraging, it is clear that more realistic assumptions will lead to a deterioration of the beam quality. This could generate beam losses with potentially

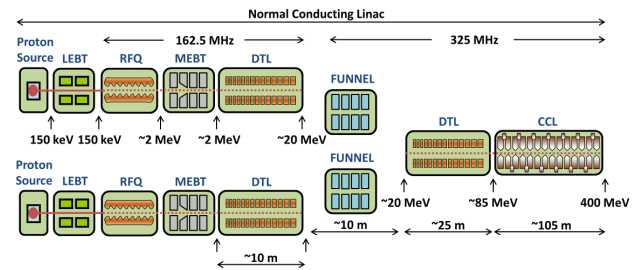


Figure 4: General layout of the 400 MeV, 0.5 A, normal conducting linac (Option 2).

catastrophic results for such a high power machine. Consequently, alternative solutions are further investigated.

## OPTION 2

The second option maintains most design choices discussed above, but assumes a 0.5 A beam current to reduce the difficulties with both generating and transporting extreme intensity beams. To arrive at the same final beam power, a funnel is envisaged at low energy such that the average beam current is doubled. The layout of the proposed machine can be seen in Figure 4. It consists of two identical front end arms, operating at 162.5 MHz. At 20 MeV, after the first DTL tank, the funnel merges the two beams into one and matches the resulting beam into the subsequent 325 MHz, DTL. This frequency is maintained up to 400 MeV, but at 85 MeV, the structure is changed to a CCL. For the purpose of this study, the funnel was not included in the simulation and a small matching section was added instead. The resulting beam envelopes can be seen in Figure 5, while tracking results are shown in Figure 6. The input RMS emittance is  $0.75 \pi$ .mm.mrad transversely and  $2.2 \pi$ .mm.mrad longitudinally. The lower beam current allows a design with smaller beams and a better aperture clearance for equal tune depressions as in Option 1. The total emittance growth is  $\sim 20\%$  transversely and  $\sim 5\%$  longitudinally, values comparable to most modern linacs currently under operation or development.

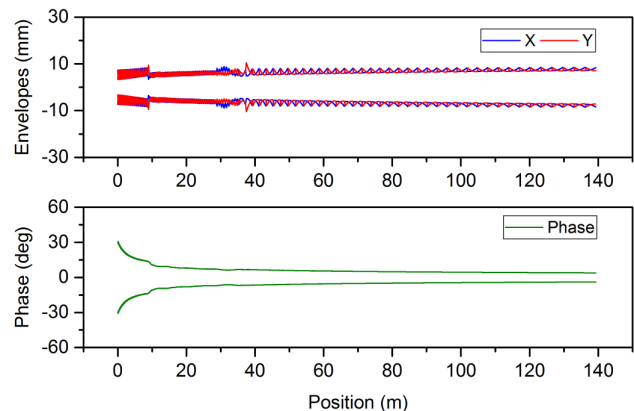


Figure 5: Beam envelopes in the Option 2 linac (2-400 MeV): horizontal (X), vertical (Y) and longitudinal (Phase).

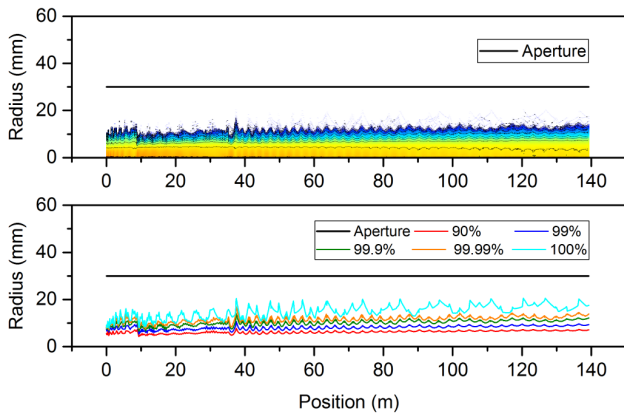


Figure 6: Radial beam density (top), and beam cross-section (bottom) evolution in the Option 2 linac (2-400 MeV).

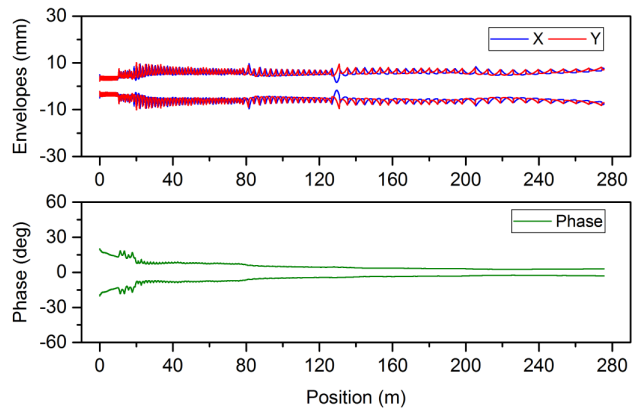


Figure 8: Beam envelopes in the Option 3 linac (5-800 MeV): horizontal (X), vertical (Y) and longitudinal (Phase).

### OPTION 3

In the third option, the beam current is further reduced to 0.25 A. The final beam power is preserved by the use of a funnel and by doubling the output beam energy to 800 MeV by means of superconducting cavities. A slightly different design approach is taken in this case. The RFQ and DTL frequency adopted is 280 MHz and the assumed RFQ output energy is 5 MeV. In the DTL, the higher frequency, the smaller aperture radius (18 mm) and the reduced accelerating gradient (2.2-2.4 MV/m), lead to a smaller level of dissipated power (0.9 MW in the first tank) and reduced thermal stress. The synchronous phase is ramped from -42 to -35 degrees.

As in the previous example, a funnel is used at ~20 MeV and is fully implemented in the simulation. The design is based on previous studies [7–9] and each arm consists of two 8 degree and one 4 degree septum dipole magnets, doublet quadrupoles and buncher cavities as well as a common 2 degree, 280 MHz deflector cavity which bends the beams alternately in opposite directions so the merged beams arrive on axis for the next structure. After the funnel, 560 MHz superconducting elliptical cavities are used to accelerate the beam to the final energy. Distributed over four sections, the cavities have accelerating gradients of 10-15 MV/m, synchronous phases from -33 to -21 degrees and employ doublet focusing. Further details are given in Figure 7.

Figure 8 shows the beam envelopes from 5 to 800 MeV while Figure 9 shows the tracking results when assuming a uniform distribution with an input rms emittance of

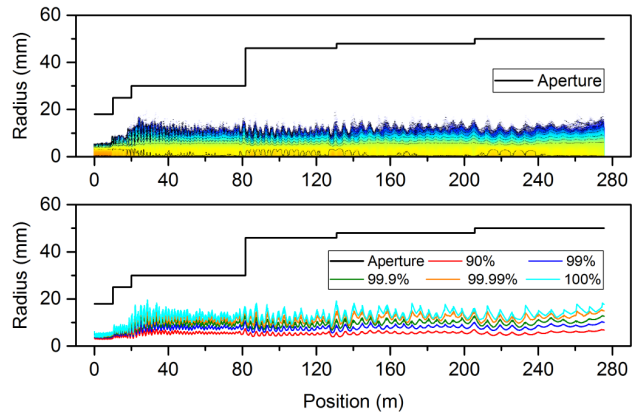


Figure 9: Radial beam density (top), and beam cross-section (bottom) evolution in the Option 2 linac (5-800 MeV).

0.5  $\pi$ .mm.mrad transversely and 0.4  $\pi$ .mm.mrad longitudinally [3]. The lower beam current and the use of large aperture superconducting cavities allow larger pipe to beam ratios and consequently more safety margins. On the other hand, the emittance growth is ~40% transversely and ~150% longitudinally, potentially caused by the multiple transitions and the use of a funnel. Further optimisation and corrections might therefore be necessary.

### CONCLUSIONS AND OUTLOOK

While many questions remain, this study uses existing concepts and accelerating structures to demonstrate that beam dynamics solutions are available to accommodate large emittances and handle difficulties involved in designing extreme intensity machines. Numerous further studies are needed - in particular beam collimation and loss control, which at high energy must be less than one part in  $10^6$  to allow hands-on-maintenance. In addition, unconventional methods for high current generation are being considered. One promising avenue is adopting well-developed ideas routinely employed in generating multi-Ampere electron beams, for proton applications, like continuous or discrete annular beams. However, these ideas will need to be investigated further [10].

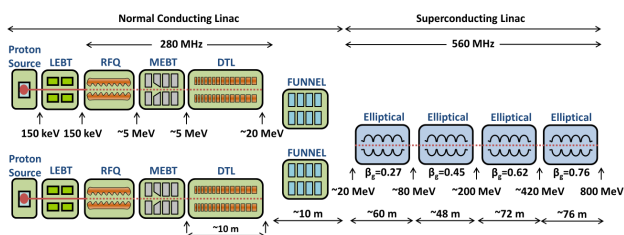


Figure 7: General layout of the 800 MeV, 0.25 A, superconducting linac (Option 3).

## REFERENCES

- [1] J. Galambos, “SNS performance and the next generation of high power accelerators”, in *Proc. of PAC’13*, Pasadena, CA, USA, 2013, paper FRYAA1, pp. 1443-7.
- [2] S. Cousineau, “High power proton facilities: operational experience, challenges, and the future”, in *Proc. of IPAC’15*, Richmond, VA, USA, 2015, paper FRYGB1, pp. 4102-6.
- [3] G. P. Lawrence and T. P. Wangler, “Integrated normal conducting/superconducting high-power proton linac for the APT project”, in *Proc. of PAC’97*, Vancouver, BC, Canada, 1997, paper 5W020, pp. 1156-8.
- [4] U. Ratzinger *et al.*, “A pulsed linac front-end for ADS applications”, in *Proc. of LINAC’12*, Tel Aviv, Israel, 2012, paper THPB007, pp. 855-7.
- [5] R. Duperier *et al.*, “CEA Saclay codes review for high intensities linacs computations”, in *Proc. of ICCS’02*, Amsterdam, Netherlands, 2012, pp. 411-8.
- [6] J. H. Billen and H. Takeda, “Parmila documentation”, LANL, Los Alamos, NM, USA, Rep. LA-UR-98-4478, 1998.
- [7] S. Nath, “Funneling in LANL high intensity linac designs”, in *AIP Conference Proceedings 346*, Las Vegas, NV, USA, 1994, p. 390.
- [8] C. R. Prior, “Funnel studies for the European Spallation Source”, RAL, Harwell, UK, Rep. ESS-99-96-A, 1999.
- [9] G. H. Rees, “Funnelling of two, 100 mA proton beams at 20.8 MeV”, *RAL Internal Report*, 2015.
- [10] I. V. Konoplev *et al.*, in *Phys. Rev. Lett.*, vol. 96, p. 035002, 2006.